"Defects in Crystals", edited by E. Mizera (World Scientific, Singapore, 1988), pp. 239-261. Proceedings of the 8th International School on Defects in Crystals, Szczyrk, Poland, 22-29 May 1988.

OXYGEN-RELATED THERMAL DONORS IN SILICON

C.A.J.Ammerlaan, H.H.P.Th.Bekman, T.Gregorkiewicz(*)

Natuurkundig Laboratorium der Universiteit van Amsterdam
Valckenierstraat 65, 1018 XE Amsterdam, The Netherlands

ABSTRACT

More than 30 years ago it was discovered that n-type electrical conductivity can be produced in silicon crystals by heat treatment. Early experiments showed that the process of donor formation is related to the presence of oxygen impurities. The precise nature and properties of the donor centres remained unclear for a long time. A tremendous research effort, mainly experimental but also theoretical, has been spent on this process of donor formation. The present paper reviews the studies of thermally-induced donors by electrical resistivity measurements, optical absorption, electron paramagnetic resonance, and electron nuclear double resonance. The main physical properties and detailed structural information on the thermal donors are revealed by these experiments.

1. INTRODUCTION

As early as 1954 it was discovered that heat treatment to modest temperatures in the 400-500 °C range of silicon crystals can produce, or enhance, n-type electrical conductivity in these crystals. The added conduction band electron concentration can exceed 10^{16} per cm^3. This, obviously important, phenomenon has since been studied in detail with the aim of learning the precise physical properties and atomic nature of the responsible donor centres. Both experimental[1-34] and theoretical[35-42] methods of study have been employed, the former sofar being the more revealing. The experimental studies have included all relevant techniques, such as electrical resistivity[1-4], optical absorption[5-11], electron paramagnetic resonance[12-19], electron nuclear double resonance[20-25], Hall effect[26-27], deep level transient spectroscopy[28-30], photo thermal ionisation spectroscopy[31-34], etc. Experiments and results of the first four methods will be reviewed in this paper. On the basis of the results a detailed knowledge of the properties and structure of the thermal donor centres will be obtained.

2. ELECTRICAL RESISTIVITY

The creation of thermal donors is most easily monitored by the room-temperature electrical conductivity of the silicon samples. The thermal donors bind the electron in shallow ground states which are ionised at room temperature. On carrying out a heat treatment the concentration of electrons in the conduction band will increase. Starting from p-type silicon, a p- to n-type conversion can take place. It was found in the early experiments that the formation of the thermal donors is related to the presence of oxygen as an impurity in the silicon crystals. The production of thermal donors is observed without exception to occur in Czochralski silicon, pulled from the melt in a quartz crucible. These silicon crystals are known to contain up to 2×10^{18} oxygen atoms per cm^3. On the other hand, in float zoned silicon, containing about 10^{15} oxygen atoms per cm^3, thermal donor formation is not observable. A typical dependence upon heat-treatment time of the added electron concentration is shown in figure 1. The thermal donor

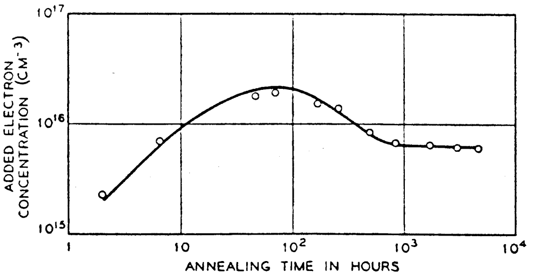

Figure 1. Increase in electron concentration resulting from annealing at 450 °C of Czochralski silicon (after Ref. 4).

formation is most readily observed in the 400 to 500 °C temperature range. A maximum thermal donor concentration is reached in times varying from minutes to several hundreds of hours, depending on the conditions of the sample and the heat treatment. For the anneal temperature T = 450 °C the figures 2 and 3 show the dependence on oxygen concentration of the initial donor formation rate and their maximum concentration, respectively. The straight lines in these plots indicate typical 3rd and 4th order power dependences. On the basis of these results the early model for the thermal donors involved the reaction $4O_i \rightarrow (O_i)_4$. The only approximate validity of the power laws and the decrease of thermal donor concentration upon prolongation of the heat-treatment time, see figure 1, however, indicate that the whole phenomenon of thermal donor formation related to oxygen clustering will be more complex than just this only reaction. Heat treatment at temperatures above 500 °C destroys the thermal donor centres.

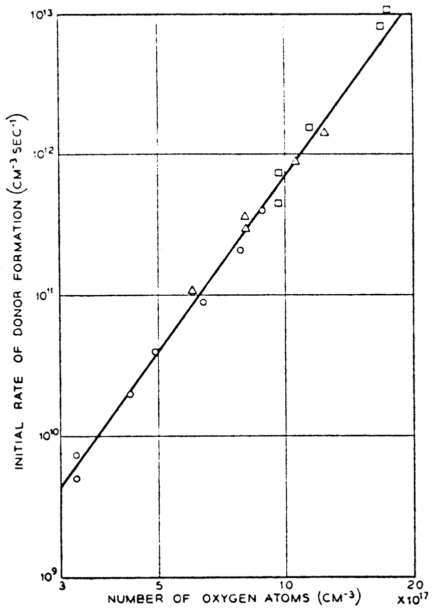

Figure 2. The initial rate of thermal donor formation in silicon as a function of the interstitial oxygen concentration, annealing temperature 450 °C (after Ref. 4).

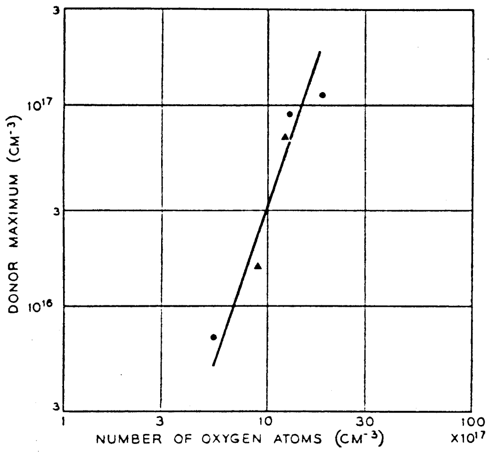

Figure 3. The maximum concentration of thermal donors in silicon as a function of the interstitial oxygen concentration, annealing temperature 450 °C (after Ref. 4).

3. OPTICAL ABSORPTION

Optical absorption spectra in the near-infrared related to the presence of thermal donors in silicon are shown in the figures 4 and 5. Several important conclusions can be drawn from these results. The absorptions are understood as excitations from the ground state to excitation levels in a hydrogenic series, well described by the effective-mass theory. For the neutral thermal donors, as shown in figure 4, nine separate series are distinguished. They correspond to different species of thermal donors. The ground state energy of each species depends, through the central-cell correction, on the precise structure of the thermal donor core. The ground state binding energies are slightly different for the nine species which are identified by the infrared absorption. Figure 4 gives the absorption spectra measured after 1, 8 and 72 hours of heat treatment at 450 °C, respectively. It is seen that upon prolongation of the heat treatment the species with the more shallow donor character develop to higher relative intensity. For suitable conditions of doping and temperature the thermal donors can exist in the positively charged ionised state. A second series of effective-mass states and transitions is then observable, as shown in figure 5. The electron is bound in the double charge of the donor core with binding energies near 150 meV. Since these levels are also ionised at room temperature, the thermal donors act as double donors. Values for the donor binding energies, for the first and second ionisation levels, are given in Table I.

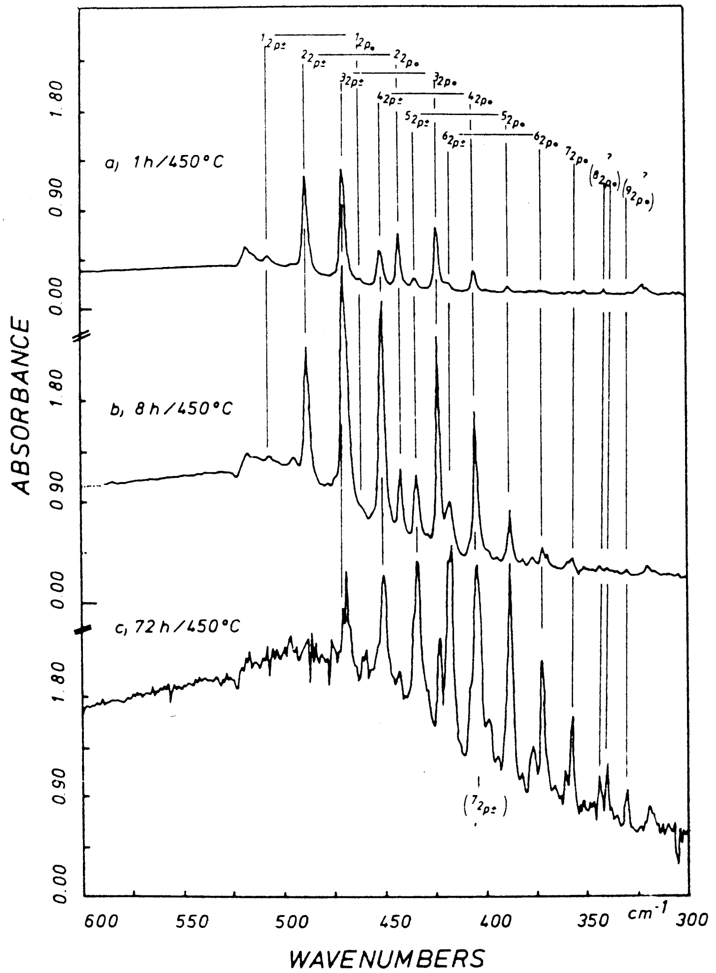

Figure 4. Absorption spectra for nine different species of neutral thermal donors TD^{0} in silicon; heat-treatment time at 450 °C a) 1 hour, b) 8 hours, c) 72 hours (after Ref. 8).

Table I. First and second ionisation energies, in meV, of thermal donor species in silicon, from Ref. 7.

Species	A	B	C	D	E	F	G	H	I
$TD^o \rightarrow TD^+$	69.1	66.7	64.4	62.1	60.1	58.0	56.2	54.3	52.9
$TD^+ \rightarrow TD^{2+}$	156.3	150.0	144.2	138.5	133.1	128.5	124	121	118

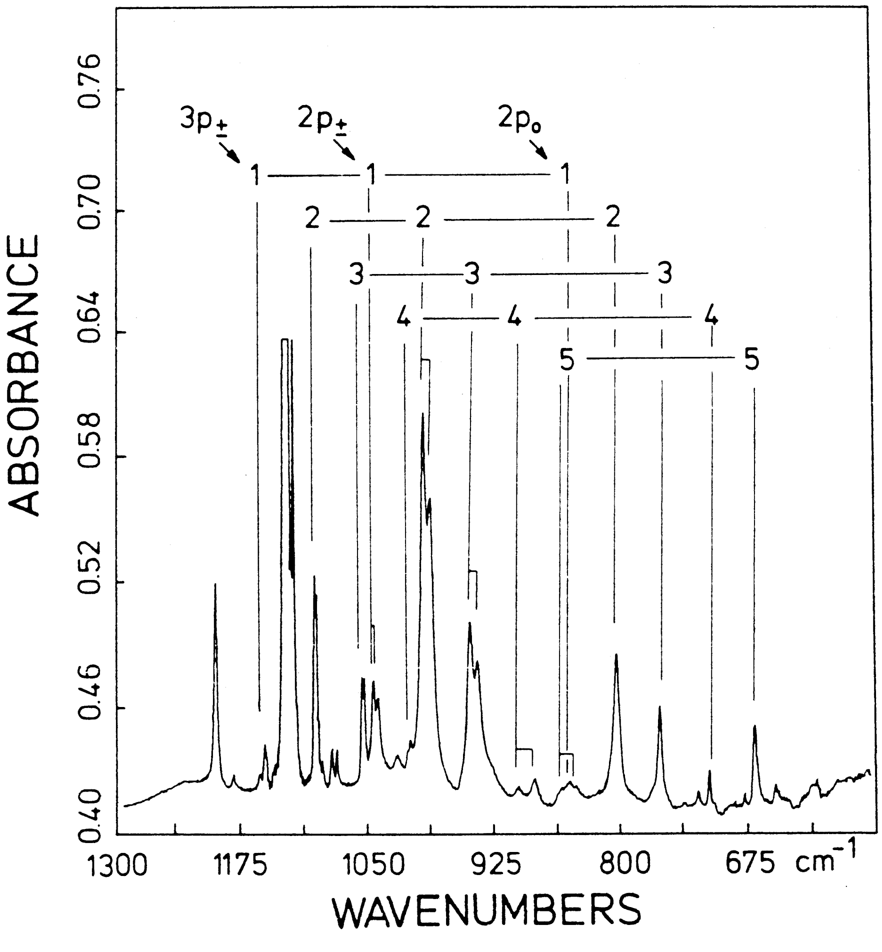

Figure 5. Absorption spectra of five different species of singly ionised thermal donors TD^+ in silicon, observable after 10 minutes heat treatment at 770 °C, followed by 2 hours at 450 °C (after Ref. 8).

4. ELECTRON PARAMAGNETIC RESONANCE

Since the charge state of thermal donors can be changed by regulating the fermi level, on may expect that thermal donors can be made to exist as paramagnetic entities. Magnetic resonance studies, which can yield detailed structural information, are then feasible. About ten years ago electron paramagnetic resonance (EPR) spectra related to thermal donors in silicon were reported. Among the various spectra initially reported, two were found to be firmly associated with thermal donors. These two spectra are labelled NL8 and NL10. In figure 6 the resonances are shown for three directions of the magnetic field. The effective g-values of the resonances are close to that for conduction band electrons, as usual for electrons bound to shallow donors.

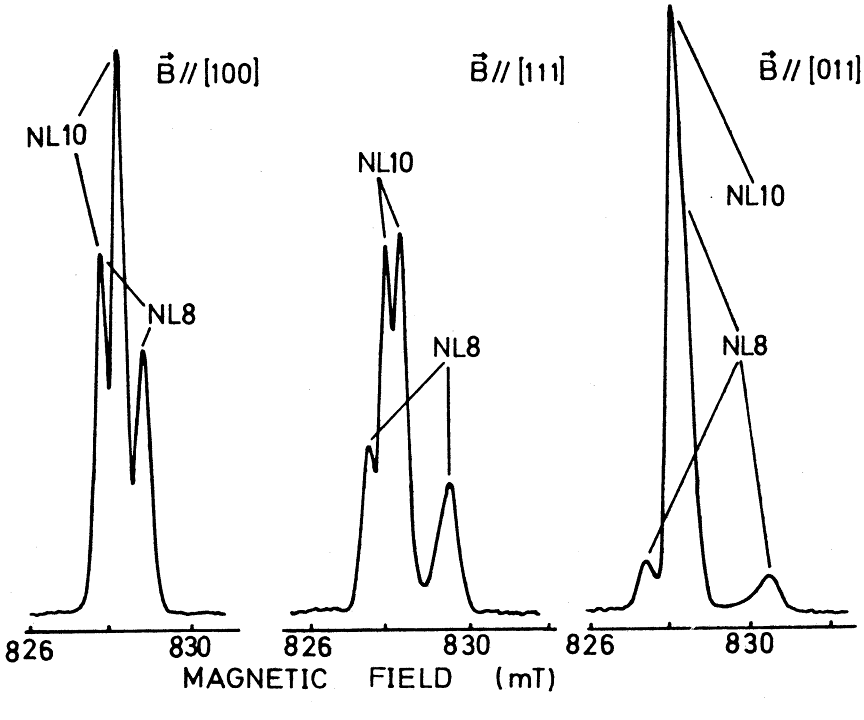

Figure 6. Electron paramagnetic resonance spectra observed in aluminium-doped Czochralski silicon after 40 hours heat treatment at 470 °C, showing the simultaneous presence of spectra NL8 and NL10.

Table II. Principal g-values g_1 (∥[100]), g_2 (∥[011]) and g_3 (∥$[0\bar{1}1]$) of the spectra NL8 and NL10 observed after short and long heat-treatment time.

Spectrum	g_1	g_2	g_3	h-t time
NL8	1.99991	1.99323	2.00091	short
	1.99991	1.99412	2.00068	long
NL10	1.99959	1.99747	1.99957	short
	1.99982	1.99799	1.99946	long

Some small anisotropy is observable in both spectra. The full angular variation is shown in figure 7 for the spectra NL8 and NL10. The spectra can be analysed with the simplest Zeeman Hamiltonian $H=\mu_B\vec{B}.\overleftrightarrow{g}.\vec{S}$, with electron spin $S=1/2$. Principal values of the g-tensor resulting from such analysis are given in Table II. The principal directions of the tensor are [100], [011] and $[0\bar{1}1]$, for principal values g_1, g_2 and g_3, respectively. These principal directions classify the spectra as belonging to a centre with orthorhombic-I symmetry. This symmetry is also unambiguously reflected in the angular dependence patterns given in figure 7. The only crystallographic point group in this class is 2mm (C_{2v}), which has a 2-fold axis along [100] and two independent mirror-planes perpendicular to [011] and $[0\bar{1}1]$. Any structural model for the thermal donors must be consistent with the symmetry established by magnetic resonance.

The variation of the resonance fields of spectra NL8 and NL10 as a function of heat-treatment time, as shown in figure 7, and of the related g-values as shown in Table II, represent an unusual phenomenon. More details of the process for the NL8 spectrum are given in figure 8. Upon prolongation of the heat treatment the centres become gradually more isotropic. From the infrared measurements it is known that thermal donors exist in the form of several distinct but very similar species. As a function of heat-treatment time the relative abundances of the separate species change. In the electron paramagnetic resonance the contributions from distinct species are unfortunately not resolved. The measured resonance is the superposition of all components. The change with time reflects the shift in relative intensities of these compo-

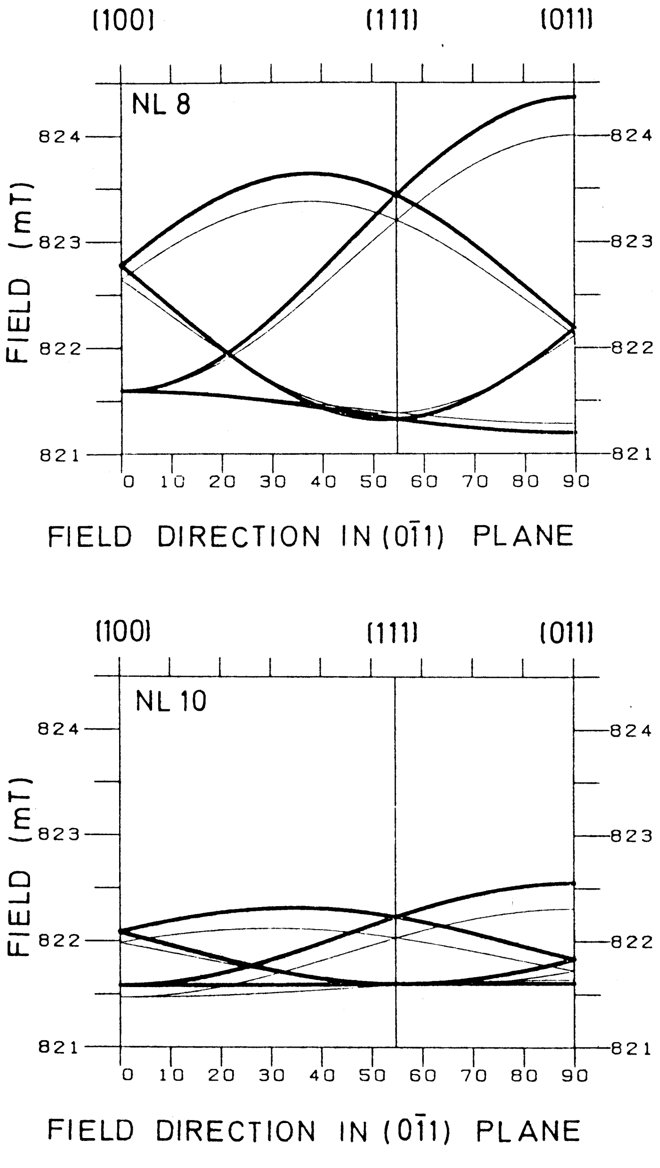

Figure 7. Resonance fields as a function of the direction of the magnetic field in the (0$\bar{1}$1)-plane for the spectra NL8 and NL10. Thick solid lines represent observations after a short heat-treatment time; thin lines give the less-anisotropic pattern observed after long heat-treatment times. Microwave frequency 23 GHz.

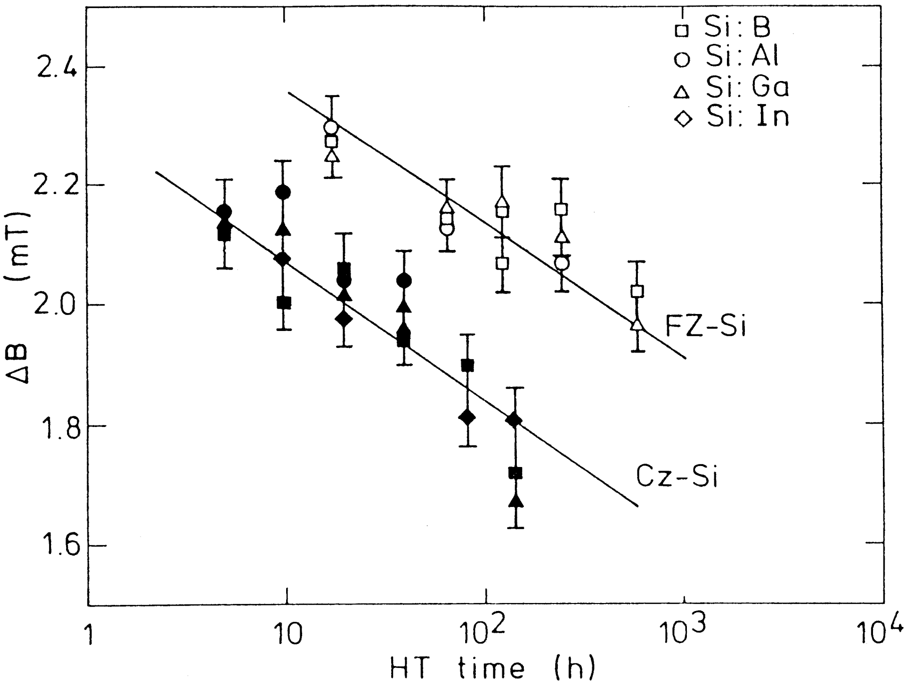

Figure 8. Separation ΔB of the two resonances for $\vec{B}\parallel[111]$ for spectrum NL8 as a function of the heat-treatment time in oxygen-diffused float-zone and Czochralski silicon of various acceptor dopings. Microwave frequency 23 GHz (after Ref. 18).

nents. Apparently the later species, which are observed as the more shallow ones in the infrared, have a more isotropic character as observed in the magnetic resonance. Figure 8 shows that for equal heat-treatment times Czochralski silicon is in a later stage of thermal donor development than oxygen-diffused float-zone silicon. This may be related to the higher oxygen concentration in the former material. For the NL10 centre similar observations were made.

Results on production of the resonance spectra are shown in figure 9 for p-type boron and aluminium doped, Czochralski and oxygen-diffused float-zone silicon. It is concluded that the nature of the acceptor has an effect on the production. On the other hand, the spectra NL8 and NL10 observed in these samples show no differences. One may conclude

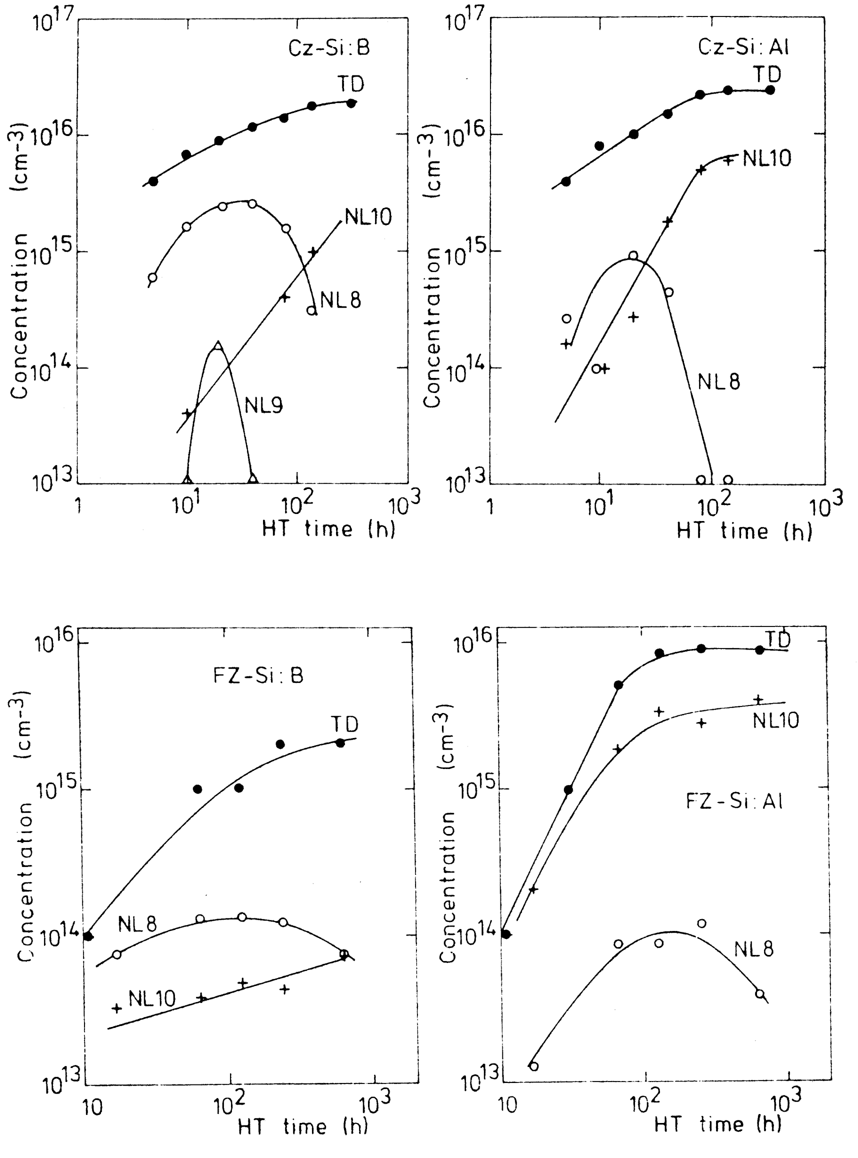

Figure 9. Production of magnetic resonance spectra NL8 and NL10 in boron and aluminium doped, Czochralski and oxygen-diffused float-zone silicon as a function of the heat-treatment time. The concentration of thermal donors monitored by resistivity changes is represented by the curves TD (after Ref. 18).

that the acceptor impurity is only indirectly involved in the formation of thermal donors, or that the resonance spectrum fails to reveal the presence of acceptors in the thermal donor structure. Systematic production studies, as shown in figure 9 for boron and aluminium, have also included the acceptors gallium and indium, and the donor phosphorus.

Usually impurities forming constituents of centres manifest themselves by hyperfine structure in the spectra. For the spectrum NL8 the search for hyperfine structure and the negative result is shown in figure 10. The p-type boron doped sample was prepared by diffusing oxygen enriched to 2.2% in the magnetic isotope ^{17}O. With the available signal quality and isotopic abundances hyperfine interactions with oxygen (^{17}O), carbon (^{13}C), boron (^{10}B and ^{11}B) and many transition elements are expected to be clearly above the noise level. The absence of hyperfine structure indicates the absence of these impurities or a weak interaction strength. Since oxygen is firmly believed to be present in the thermal donor one must conclude that the linewidth of the electron paramagnetic resonance obscures the hyperfine structure.

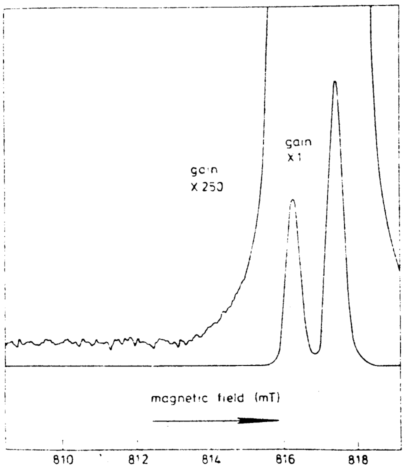

Figure 10. Paramagnetic resonance spectrum NL8 for $\vec{B} \parallel [100]$, observed in p(B) silicon, diffused with oxygen, 2.2% of isotope ^{17}O. The trace recorded with 250x increased gain does not reveal any hyperfine structure (after Ref. 13).

5. ELECTRON NUCLEAR DOUBLE RESONANCE

With the inability of electron paramagnetic resonance to reveal the expected oxygen hyperfine structure the need for enhanced resolution is apparent. Electron nuclear double resonance (ENDOR) can offer an improvement by typically three orders of magnitude. Samples were prepared by diffusing oxygen, enriched in the magnetic isotope ^{17}O, into float-zone silicon. A special technique, using a quad-elliptical infrared heating furnace, allowing the controlled introduction of oxygen into float-zone silicon under very clean conditions, was developed for this purpose. Diffusion of oxygen is carried out at a sample temperature just below the melting point for a duration of typically 14 days. The uniform introduction into 2 mm thick samples of about 4×10^{17} oxygen atoms per cm^3, with about 30% of the ^{17}O isotope, was positively verified by low-temperature high-resolution measurement of the vibrational absorption in the 9 μm band.

In such samples electron nuclear double resonance due to the oxygen nucleus was observed for the spectra NL8 and NL10. For both spectra the electron spin is $S=1/2$; the nuclear spin of the oxygen isotope is $I=5/2$. The nuclear transitions as observed in ENDOR, with the selection rules $\Delta m_S=0$, $\Delta m_I=\pm1$, are represented in the level diagram figure 11. A total of ten transitions will be possible for each nucleus. An angular plot of ENDOR transition frequencies observed for magnetic field in the $(0\bar{1}1)$-plane is shown in figure 12. The result was obtained for the NL10 thermal donor and on an EPR resonance corresponding to a single defect orientation. For a general angle in the $(0\bar{1}1)$-plane 20 transitions were measured. This number indicates that the transitions arise from two or four different oxygen nuclei. The full results, including ENDOR observed on other defect orientations, indicate that two oxygen atoms are present. For the high-symmetry directions [100] and [011] transitions coincide as a result of existing symmetry. This confirms that the two oxygen atoms are on sites related by symmetry operations of the centre. Specifically, for the 2mm symmetry of the NL8 and NL10 centres this implies that the oxygen atoms occupy sites on a mirrorplane of the defect. Several other angular dependent patterns of ENDOR frequencies were observed, with identical features of symmetry. This shows that

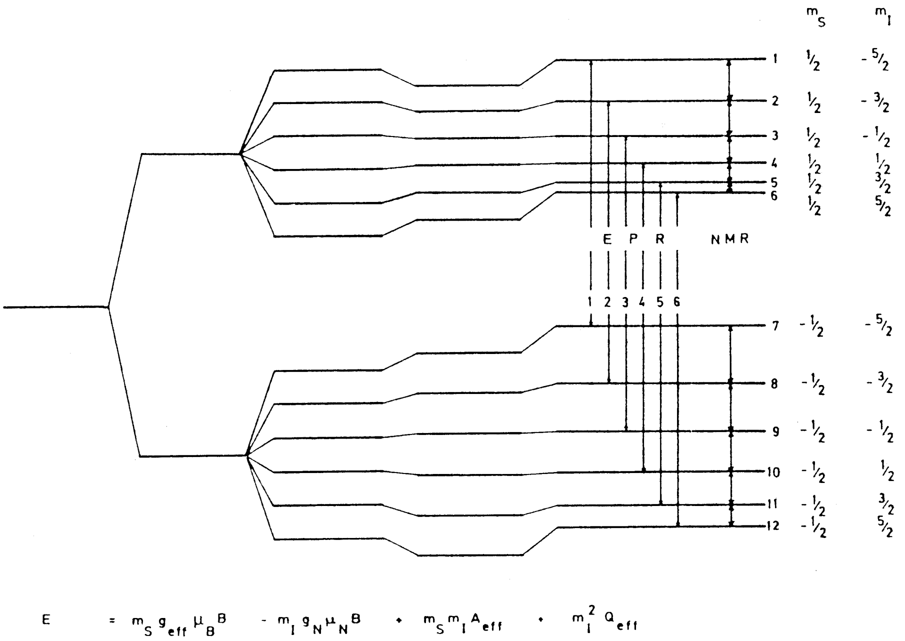

Figure 11. Schematic diagram (not to scale) of the energy levels of a system with electron spin S-1/2 and nuclear spin I-5/2. Electron spin transitions with Δm_S-±1 are observed in EPR; nuclear spin transitions with Δm_I-±1, labelled NMR, are observed in ENDOR.

other pairs of oxygen atoms are present, also in shells of sites on the same mirrorplane of the centres. The quantitative analysis of the ENDOR results uses the powerful concept of the spin Hamiltonian. For the spin system S-1/2 and I-5/2, the required terms include electron Zeeman interaction $\mu_B\vec{B}.\overleftrightarrow{g}.\vec{S}$, nuclear Zeeman interaction $g_N\mu_N\vec{B}.\vec{I}$, hyperfine interaction $\vec{S}.\overleftrightarrow{A}.\vec{I}$ and electric quadrupole interaction $\vec{I}.\overleftrightarrow{Q}.\vec{I}$. With the eigenvalues of the Hamiltonian the observed transition frequencies can be matched within the experimental error of typically 1 kHz. The elements of the coupling tensors are thereby determined with great precision. From the nuclear g-value the identity of the impurity involved follows unambiguously. This leads to the major conclusion of the presence of oxygen as constituent of the NL8 and NL10 centres. The hyperfine interaction tensors are very nearly isotropic and correspond to a

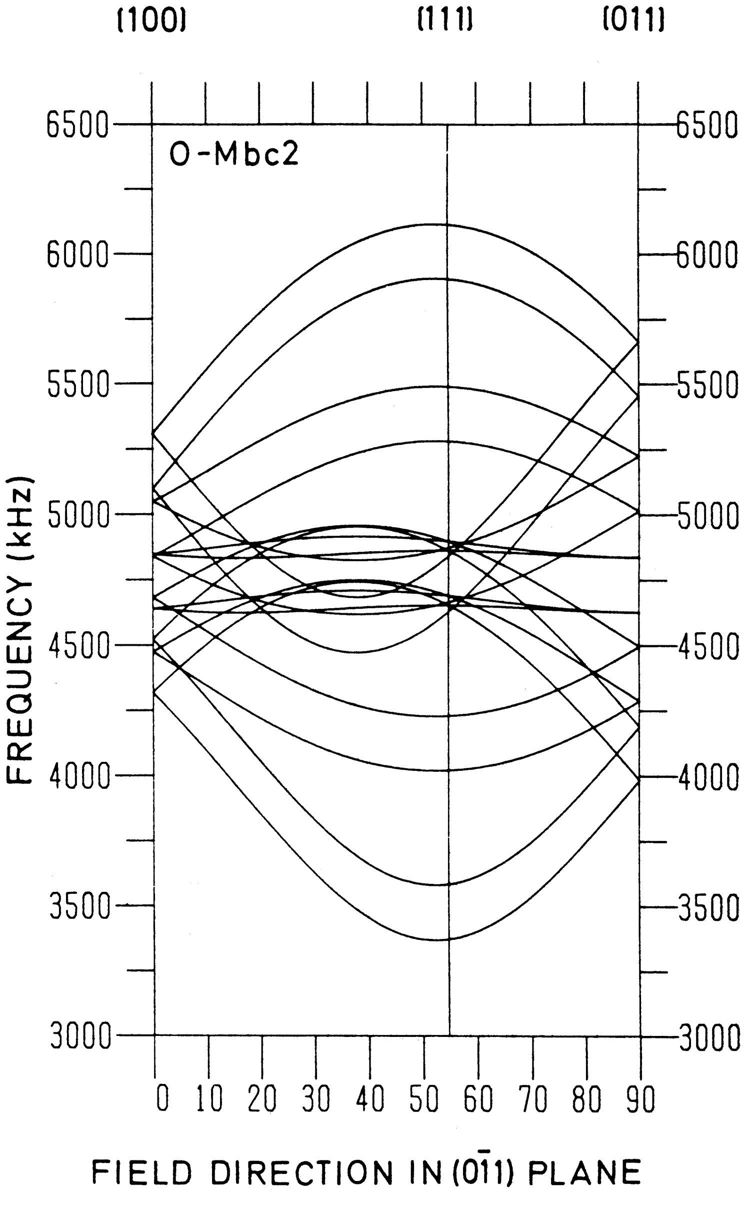

Figure 12. Computer simulation of the angular pattern, $\vec{B}$ in the (0$\bar{1}$1)-plane, of oxygen ENDOR frequencies observed on the EPR of a single NL10 orientation (after Ref. 25).

low spin density. This is consistent with the extended character of the wave function of the shallow bound electron. The anisotropy as seen in figure 12 is mainly due to the quadrupole interaction. Since the unpaired spin density is low, the quadrupole effect must arise from valence charge redistribution. Analysis shows that the observed tensors are consistent with the normal sites of interstitial oxygen, in a bond-centered plane, displaced from the axis.

The oxygen ENDOR is found at frequencies near, and roughly symmetrical above and below the nuclear Zeeman frequency of the ^{17}O isotope. But also at much higher frequencies ENDOR was observed on the NL10 paramagnetic resonance spectrum. The angular dependence of one pattern is given in figure 13. The ten branches in the pattern correspond to the transitions within the levels of a single nucleus with spin $I=5/2$. With the spin Hamiltonian analysis the nucleus is identified through its nuclear g-factor as the mass-27 isotope of aluminium. The position of the aluminium atom is on the 2-fold axis of the NL10 centre. Very surprisingly for aluminium nuclei also ENDOR frequency patterns were measured of the same symmetry type as for oxygen. Straightforward interpretation would imply the presence of two aluminium nuclei in the centre. Since such conclusion is hard to accept, a careful examination of this ENDOR was carried out by the field stepped ENDOR method. In field stepped ENDOR, scans through the NMR transition are made for several values of the magnetic field near the centre of the EPR line. This results in a magnetic field determination of the magnetic resonance with optimum resolution. Results of such measurements for wo related aluminium ENDOR lines are summarised in figure 14. It is observed that the ENDOR lines result from two magnetic resonances which are different by about 0.04 mT. The resonance branch, which in regular EPR appears as one line, is actually composed of two separate resonance fields. The splitting implies a monoclinic-I symmetry of the pattern and thus of the corresponding centre. The degree of distortion of the thermal donors from orthorhombic towards the lower monoclinic symmetry is small and remains unobservable in the regular electron paramagnetic resonance spectrum. The true symmetry of some of the centres is however monoclinic-I, crystallographic point group m. This symmetry allows the

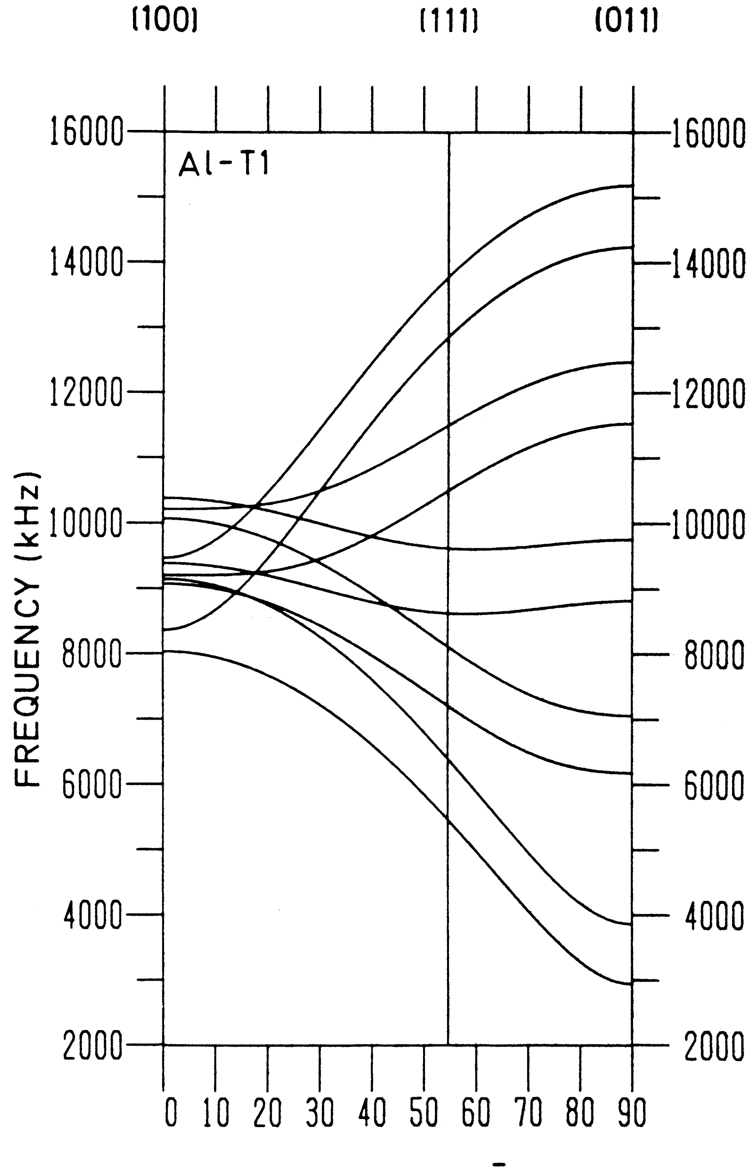

Figure 13. Computer simulation of the angular pattern, $\vec{B}$ in the (0$\bar{1}$1)-plane, of aluminium ENDOR frequencies observed on the EPR of a single NL10 orientation (after Ref. 25).

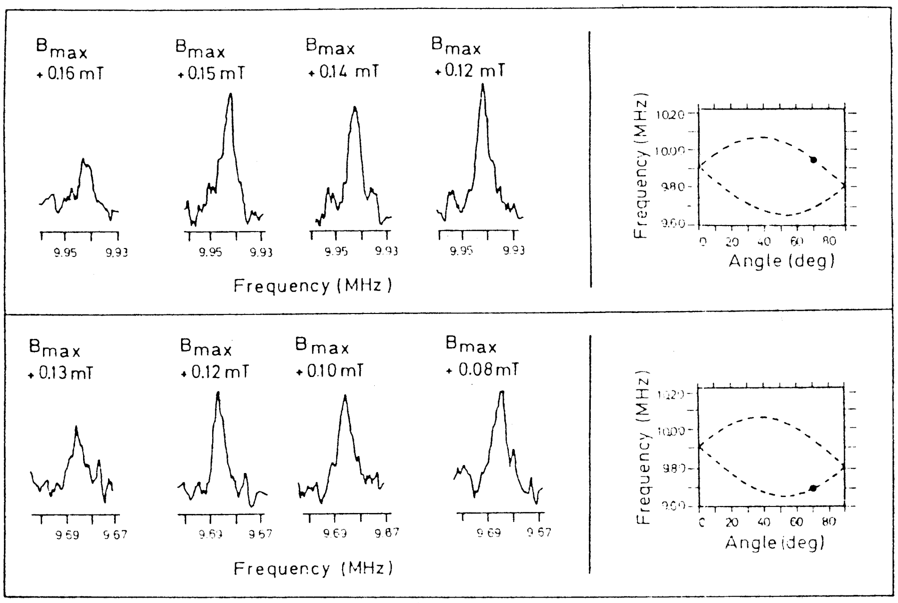

Figure 14. Illustration of the field stepped ENDOR method, applied to two ^{27}Al ENDOR transitions of one loop and same magnetic field direction, as shown in the right panels. Results on the left show the magnetic field dependence of the ENDOR signal. Field B_{max} is the centre of the EPR line (after Ref. 25).

thermal donors to grow by accepting oxygen atoms one-by-one on the mirroplane m. Such a mechanism eliminates the need for the unlikely situation of thermal donors existing with even numbers of oxygen atoms only and growing by addition of oxygen atoms in pairs.

The method of field stepped ENDOR was applied systematically to find the best magnetic resonance field for observation of the ENDOR lines. Figure 15 illustrates some results. For example, in this figure it is demonstrated that the ENDOR transition labeled 1 belongs to a component in the EPR with higher field than the central field B_{max}, whereas transition 8 is associated with a low field component. In this way the ENDOR lines can be related to the components of the EPR line. The resolution enhancement of field stepped ENDOR just allows to accomplish the sorting of tensors into groups. The components in the EPR have a

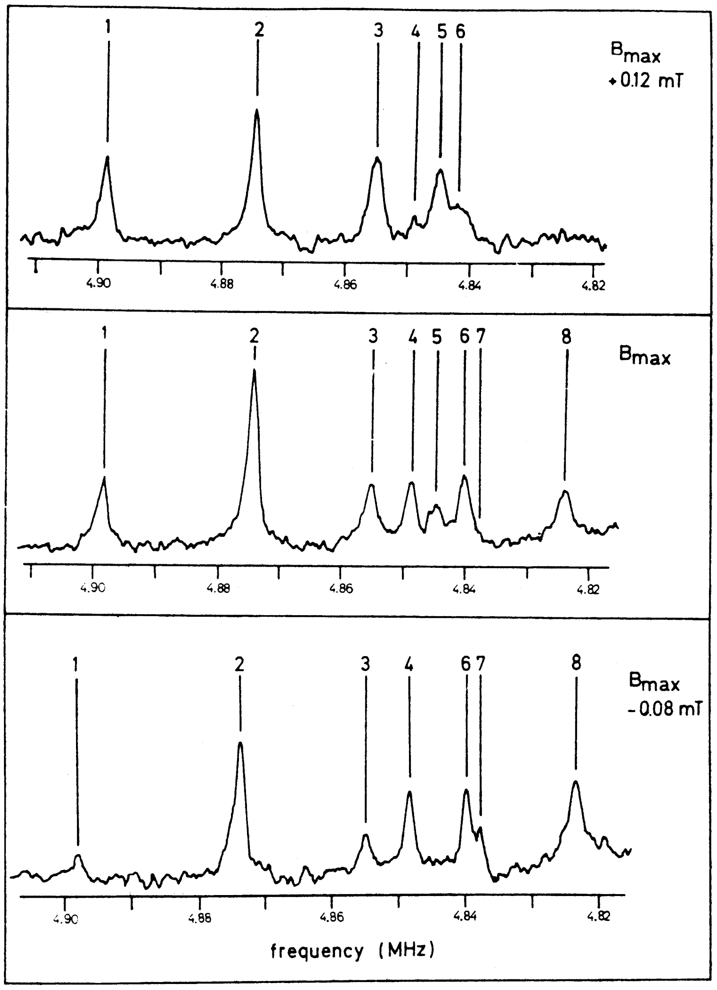

Figure 15. Illustration of the field stepped ENDOR method, applied to eight ^{17}O ENDOR transitions. Results show the different magnetic field values for best observation of the ENDOR, allowing the decomposition of the EPR into components belonging to separate species (after Ref. 25).

correspondence with the existing species of thermal donors. The correlation of ENDOR with components in the EPR thus corresponds to assignment of hyperfine and quadrupole tensors from shells of nuclei to the distinct species of the thermal donors.

6. CONCLUSION

Probably the most astonishing conclusion is that in spite of the tremendous research effort still no atomic model is established accounting in an indisputable way for the observations on the formation and properties of the thermal donors. Over the years many proposals were put forward[43-51]. Most of the models are of orthorhombic symmetry to comply with the conclusions of electron paramagnetic resonance studies. Recent high-resolution measurements by the field stepped ENDOR method, as discussed in the previous paragraph, have shown that the symmetry constraint for the NL10 centre can be relaxed to monoclinic.

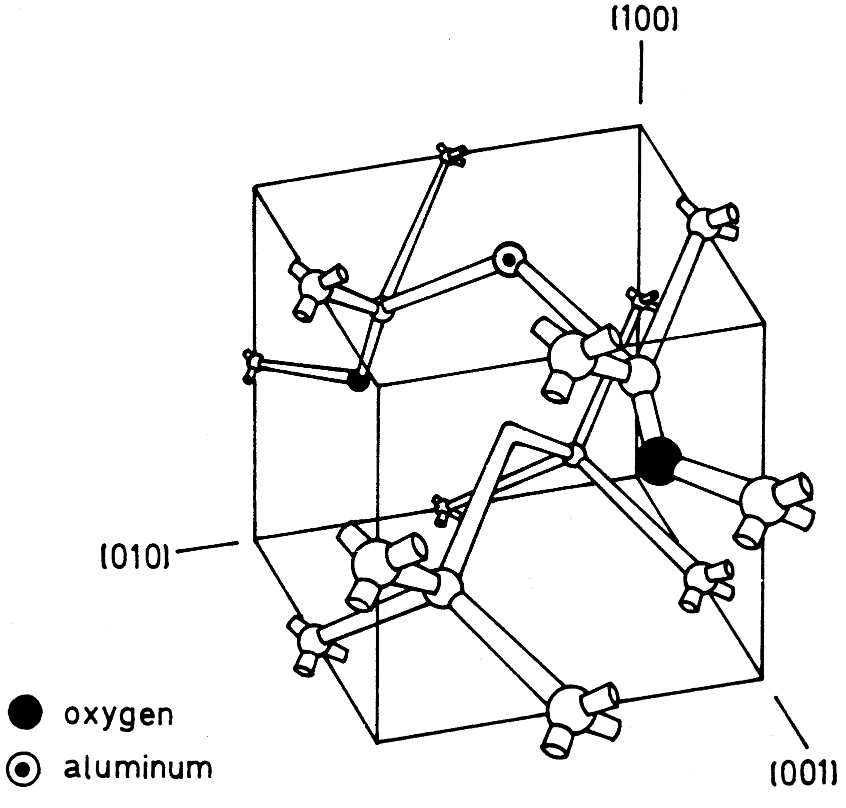

Figure 16. A structural model for an NL10 centre incorporating one aluminium and two oxygen atoms (after Ref. 25).

A model consistent with the presently available structural information for the NL10 centre is presented in figure 16. This basic structure has an aluminium atom on the [100] two-fold axis of the centre and two oxygen atoms on the (011)-plane. The observation of the NL10 spectrum in silicon doped with acceptors boron, gallium or indium, however, proves that aluminium can not be a crucial constituent of the centre. The formation of the later species proceeds by the addition of single oxygen atoms in the (011)-plane. The symmetry may then alternate between orthorhombic and monoclinic.

Several aspects are still open for further verification. Among these are the confirmation of a vacancy in the centre and the shallow donor character of the proposed structure. Further improvement of the resolution in magnetic resonance would also be extremely useful to establish the details in the structure of these important oxygen clusters.

REFERENCES

Electrical resistivity

1. Fuller, C.S., Ditzenberger, J.A., Hannay, N.B. and Buehler, E., Phys. Rev. **96**,833(1954).
2. Fuller, C.S., Ditzenberger, J.A., Hannay, N.B. and Buehler, E., Acta Met. **3**,97(1955).
3. Fuller, C.S. and Logan, R.A., J. Appl. Phys. **28**,1427(1957).
4. Kaiser, W., Frisch, H.L. and Reiss, H., Phys. Rev. **112**,1546(1958).

Optical absorption

5. Hrostowski, H.J. and Kaiser, R.H., Phys. Rev. Lett. **1**,199(1958).
6. Wruck, D. and Gaworzewski, P., Phys. Stat. Sol. (a) **56**,557(1979).
7. Pajot, B., Compain, H., Lerouille, J. and Clerjaud, B., Physica **117**B&**118**B,110(1983).
8. Oeder, R. and Wagner, P., in "Defects in Semiconductors II", (North-Holland, New York, 1983), p.171.
9. Stavola, M., Lee, K.M., Nabity, J.C., Freeland, P.E. and Kimerling, L.C., Phys. Rev. Lett. **54**,2639(1985).
10. Stavola, M. and Lee, K.M., in "Oxygen, Carbon, Hydrogen and Nitrogen in Crystalline Silicon", (Materials Research Society, Pittsburgh, 1986), p. 95.
11. Wagner, P., in "Oxygen, Carbon, Hydrogen and Nitrogen in Crystalline Silicon", (Materials Research Society, Pittsburgh, 1986), p. 125.

Electron paramagnetic resonance

12. Graff, K., Hilgarth, J. and Neubrand, H., in "Semiconductor Silicon 1977", (Electrochem. Soc., Princeton, 1977), p. 575.

13. Muller, S.H., Sprenger, M., Sieverts, E.G. and Ammerlaan, C.A.J., Solid State Commun. 25,987(1978).
14. Muller, S.H., Sieverts, E.G. and Ammerlaan, C.A.J., in "Defects and Radiation Effects in Semiconductors 1978", (Inst. Phys., Bristol, 1979), p.297.
15. Suezawa, M., Sumino, K. and Iwaizumi, M., J. Appl. Phys. 54,6594 (1983).
16. Lee, K.M., Trombetta, J.M. and Watkins, G.D., in "Microscopic Identification of Electronic Defects in Semiconductors", (Materials Research Society, Pittsburgh, 1985), p. 263.
17. Wörner, R. and Schirmer, O.F., Phys. Rev. B 34,1381(1986).
18. Gregorkiewicz, T., Wezep, D.A. van, Bekman, H.H.P.Th. and Ammerlaan, C.A.J., Phys. Rev. B 35,3810(1987).
19. Bekman, H.H.P.Th., Gregorkiewicz, T., Wezep, D.A. van and Ammerlaan, C.A.J., J. Appl. Phys. 62,4404(1987).

Electron nuclear double resonance

20. Wezep, D.A. van, Gregorkiewicz, T., Bekman, H.H.P.Th. and Ammerlaan, C.A.J., Materials Science Forum 10-12,1009(1986).
21. Michel, J., Niklas, J.R., Spaeth, J.-M. and Weinert, C., Phys. Rev. Lett. 57,611(1986).
22. Michel, J., Niklas, J.R. and Spaeth, J.-M., in "Oxygen, Carbon, Hydrogen and Nitrogen in Crystalline Silicon", (Materials Research Society, Pittsburgh, 1986), p. 111.
23. Gregorkiewicz, T., Wezep, D.A. van, Bekman, H.H.P.Th. and Ammerlaan, C.A.J., Phys. Rev. Lett. 59.1702(1987).
24. Michel, J., Niklas, J.R. and Spaeth,,J.-M., in "Defects in Electronic Materials" (Materials Research Society, Pittsburgh, 1988).
25. Gregorkiewicz, T., Bekman, H.H.P.Th. and Ammerlaan, C.A.J., Phys. Rev. B 38 (1988).

Hall effect

26. Morin, F.J., Maita, J.P., Shulman, R.G. and Hannay, N.B., Phys. Rev. 96,833(1954).
27. Gaworzewski, P. and Schmalz, K., Phys. Stat. Sol. (a) 55,699(1979).

Deep level transient spectroscopy

28. Farmer, J.W., Meese, J.M., Henry, P.M. and Lamp, C.D., J. Electron. Mater. 14a,639(1985).
29. Benton, J.L., Lee, K.M., Freeland, P.E. and Kimerling, L.C., J. Electron. Mater. 14a,647(1985).
30. Henry, A., Pautrat, J.L., Magnea, N. and Saminadayar, K., in "Oxygen, Carbon, Hydrogen and Nitrogen in Crystalline Silicon", (Materials Research Society, Pittsburgh, 1986), p. 153.

Photo thermal ionisation spectroscopy

31. Navarro, H., Griffin, J., Weber, J. and Genzel, L., Solid State Commun. 58,151(1986).
32. Griffin, J.A., Navarro, H., Weber, J. and Genzel, L., Materials Science Forum 10-12,997(1986).
33. Griffin, J.A., Navarro, H. and Genzel, L., in "Oxygen, Carbon, Hydrogen and Nitrogen in Crystalline Silicon", (Materials Research

Society, Pittsburgh, 1986), p. 139.

34. Griffin, J.A., Navarro, H., Weber, J., Genzel, L., Borenstein, J.T., Corbett, J.W. and Snyder, L.C., J. Phys. C: Solid State Phys. **19**,L579(1986).

Theory

35. Wada, K., Phys. Rev. B **30**,5884(1984).
36. Robertson, J. and Ourmazd, A., Appl. Phys. Lett. **46**,559(1985).
37. DeLeo, G.G., Milsted, C.S. and Kralik, J.C., Phys. Rev. B **31**,3588 (1985).
38. LaPorta, C.S., Kimball, J.C., Borenstein, J.T. and Corbett, J.W., J. Phys. C: Solid State Phys. **19**,L627(1986).
39. Snyder, L.C. and Corbett, J.W., in "Oxygen, Carbon, Hydrogen and Nitrogen in Crystalline Silicon", (Materials Research Society, Pittsburgh, 1986), p. 207.
40. Tan, T.Y., Kleinhenz, R. and Schneider, C.P., in "Oxygen, Carbon, Hydrogen and Nitrogen in Crystalline Silicon", (Materials Research Society, Pittsburgh, 1986), p. 195.
41. Borenstein, J.T. and Corbett, J.W., in "Oxygen, Carbon, Hydrogen and Nitrogen in Crystalline Silicon", (Materials Research Society, Pittsburgh, 1986), p. 159.
42. Borenstein, J.T., Peak, D. and Corbett, J.W., in "Oxygen, Carbon, Hydrogen and Nitrogen in Crystalline Silicon", (Materials Research Society, Pittsburgh, 1986), p. 173.

Models

43. Kaiser, W., Frisch, H.L. and Reiss, H., Phys. Rev. **112**,1546(1958).
44. Helmreich, D. and Sirtl, E., in "Semiconductor Silicon 1977", (Electrochem. Soc.. Princeton, 1977), p. 626.
45. Gösele, U. and Tan, T.Y., Appl. Phys. A **28**,79(1982).
46. Pajot, B., Compain, H., Lerouille, J. and Clerjaud, B., Physica **117B&118B**,110(1983).
47. Newman, R.C., Oates, A.S. and Livingston, F.M., J. Phys. C: Solid State Phys. **16**,L667(1983).
    Newman, R.C., J. Phys. C: Solid State Phys. **18**,L967(1985).
48. Stavola, M. and Snyder, L.C., in "Defects in Silicon", (Electrochem. Soc., Pennington, 1983), p. 61.
    Snyder, L.C. and Corbett, J.W., J. Electron. Mater. **14a**,693(1985).
49. Henry, P.M., Farmer, J.W. and Meese, J.M., Appl. Phys. Lett. **45**, 454(1984).
50. Keller, W.W., J. Appl. Phys. **55**,3471(1984).
51. Ourmazd, A., Schröter, W. and Bourret, A., J. Appl. Phys. **56**,1670 (1984).

(*) On leave from the Institute of Physics of the Polish Academy of Sciences, Al.Lotników 32/46, 02-668 Warsaw, Poland.